Sensor Applications

A Wearable Sweat Rate Sensor with Adaptive Sweat Ion Concentration Calibration

Mohammad Shafiqul Islam[1,2], Sangwon Cha[1,2*], Wenxin Cai[2,3], Munia Ferdoushi[1,2*], Yasser Khan[1,2**]

[1]*Department of Electrical and Computer Engineering, University of Southern California, Los Angeles, CA 90089, USA*
[2]*The Institute for Technology and Medical Systems (ITEMS), Keck School of Medicine, University of Southern California, Los Angeles, CA 90033, USA*
[3]*Mork Family Department of Chemical Engineering and Materials Science, University of Southern California, Los Angeles, CA 90089, USA*
[*] *Member, IEEE*
[**] *Senior Member, IEEE*

Abstract—Wearable sensors for continuous physiological biomarker monitoring offer a non-invasive and personalized approach to healthcare. Sweat, as a readily accessible biofluid, serves as a valuable medium for biomarker detection. However, accurate biomarker analysis relies on precise sweat rate measurements, as sweat concentration and secretion rates are interdependent. To address this, it is critical to calibrate sweat ion concentration to enhance the accuracy of sweat rate monitoring. Moreover, the distribution of sweat glands varies across different body regions, necessitating application-specific design modifications for wearable sweat rate sensors. Effective sensor implementation requires adaptability in design while ensuring compatibility with scalable fabrication techniques. In this work, we present a digital fabrication method that allows for easy customization and large-area manufacturability. A key advancement in our approach is the integration of secondary capacitive sensing to continuously monitor sweat ion concentration, which is incorporated into real-time sweat rate calculations. This calibration technique enhances measurement precision by accounting for fluctuations in sweat composition. Additionally, we developed customized readout electronics and a mobile application for real-time sweat rate visualization, enhancing user accessibility and convenience. By incorporating sweat ion concentration calibration through capacitive sensing, our sensor system significantly improves the accuracy and reliability of sweat rate measurements, advancing real-time perspiration monitoring for personalized health applications.

Index Terms—Sweat Rate, Sweat Sensing, Capacitive Sweat Rate Sensor, Sweat Concentration, Digital Design, Inkjet Printing.

I. INTRODUCTION

Sweat is a readily available medium rich in information, making it a primary focus for wearable sensors in recent years. The biomarkers found in sweat, including ions, metabolites, and hormones, can provide valuable insights into an individual's hydration status and thermoregulation [1], [2]. Sweat analysis has further applications in drug abuse testing, along with monitoring of therapeutic drugs [3] and progression of various illnesses, such as cystic fibrosis and Wilson's disease [4]. However, sweat contents are heavily affected by Sweat Rate (SR) [5]. Moreover, SR heavily varies based on environmental conditions, physical activity, underlying pathologies, and sweat stimulation methods [6]. Hence, SR sensing is crucial for both monitoring hydration status and accurately interpreting the sweat biomarker profiling for clinical and sports applications.

Traditional sweat sensing methods rely on observation of either body mass change [7] or absorbent pad techniques [8]. Medical grade sweat sensing system Q-Sweat works based on moisture content change [9] but is expensive and requires trained personnel to perform SR measurements. Recent years have seen a rise in wearable commercial sweat-sensing devices based on sweat-sensing patches (NiX hydration monitor) and microfluidic devices (Gatorade GX Sweat Patch) [10]. Other notable wearable solutions are based on calorimetry, hygrometry, and changes in electrical properties to correlate easily measurable quantities to SR. Calorimetric systems sense thermal flow rate but demand high power consumption to operate the heating elements [11], [12]. Humidity-based SR sensors create a pressure gradient between two humidity sensors placed at different heights from the skin [13], [14], but such a setup requires a relatively complex multilayer structure for implementation. Impedimetric SR sensors are based on changes in admittance due to sweat flow in a microfluidic channel [15], [16]. Capturing capacitance variation along parallel plates has been shown to have improved sweat sensing performance, all the while achieving low fabrication costs [17], [18]. Recent developments in power-efficient thermal actuators and precision thermistors, additive manufacturing, and printed electronics have led to the development of various wireless sweat sensors [18], [19]. However, most of the reported works do not consider sweat ion concentration changes. The fabrication method is also complex and not large-area-compatible. Most of them are not feasible for continuous real-time monitoring of human perspiration.

This work presents a digital fabrication method for developing a range of designs and capacities for inkjet-printed SR sensors. These designs can be easily adjusted to align with specific application needs and channel volume requirements. Furthermore, we offer a straightforward solution to tackle the inconsistencies in SR measurements arising from variations in sweat ion concentration. Our custom readout electronics, combined with a smartphone application, facilitate continuous monitoring of sweat rate with improved accuracy by integrating sweat concentration into SR measurements.

II. METHODS

The number of sweat glands varies in different areas of the body, requiring the sensor channel's capacity volume to adjust for precise SR measurements. Fig. 1. A shows a digital fabrication method

Corresponding author: Yasser Khan (e-mail: yasser.khan@usc.edu).

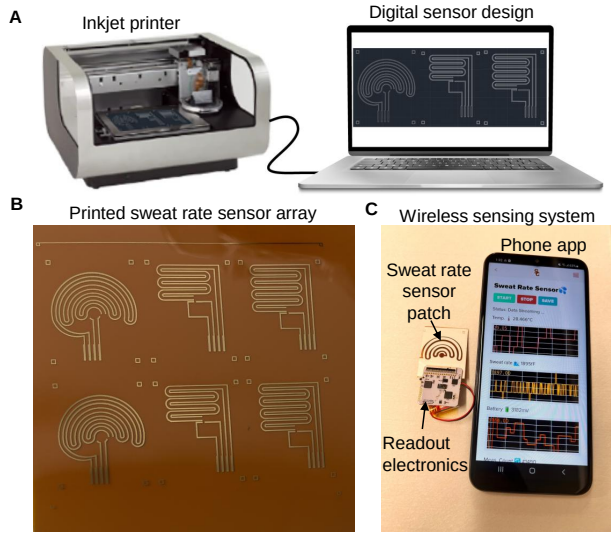

Fig. 1. **Digital fabrication of sensor array and wireless system for SR measurement**. (**A**) Digital design and inkjet printer for sensor fabrication. (**B**) Printed sensor array according to the digital design. (**C**) Sensor patch with custom-built readout electronics. The sensor is interfaced with a Nordic nRF52832 system-on-chip, which streams data to a phone application for real-time SR monitoring.

using an inkjet printer to create the sensor patch, which consists of four layers: metal electrodes, dielectric encapsulation, a microfluidic channel, and a clear cover, all designed in AutoCAD. Metal electrodes and dielectric layers are inkjet printed, while the microfluidic layers are cut with a laser. This method, illustrated in Fig. 1. B, allows for quick design changes and efficient sensor array production. Our custom electronics and mobile app enable easy use of the sensor patch in daily activities, as shown in Fig. 1. C, which features wireless data communication and display capabilities.

Our capacitive SR sensor uses a parallel plate configuration to determine SR. While the sweat flows inside the channel, the dielectric constant of the capacitance changes, and the capacitance value changes accordingly. Sweat flow rate dictates the rate at which the capacitance changes. Thus, we can correlate the change in capacitance, $\frac{dC_s(t)}{dt}$, with the sweat flow rate, $SR(t)$, by using the following equation,[18]

$$\frac{dC_s(t)}{dt} = \left(\frac{\epsilon_d \epsilon_f}{2\epsilon_f d_d d_f + \epsilon_d d_f^2} - \frac{\epsilon_d \epsilon_a}{2\epsilon_a d_d d_f + \epsilon_d d_f^2}\right) SR(t) \quad (1)$$

Here, d_d and ϵ_d are the width and dielectric constant of the encapsulation dielectric. d_f and ϵ_f are width and dielectric constant for the sweat. $d = d_f + 2d_d$ is the distance between two parallel plates as shown in Fig. 2. A. $\epsilon_a = \epsilon_0$ is the dielectric constant in the channel filled with air.

Sweat concentration varies from person to person and varies over time for each individual. The calibration curve of the capacitive SR sensor also varies depending on the sweat concentration [15], [18]. Hence, incorporating sweat concentration dependence measurement is necessary to determine the SR precisely. In this work, we introduce a secondary parallel plate capacitor at the inlet of the SR sensor patch. The dimension of this secondary capacitance is fixed, and it can determine the dielectric constant of the incoming sweat at the microfluidic channel's inlet by using $C_{fixed} = \epsilon_f A_{fixed}/d_{fixed}$. Fig. 2 B shows the two sets of capacitors, one for measuring SR and another for determining sweat ion concentration. We simulated three different designs to study the robustness of our proposed digital fabrication method. Simulation results provide insight into these design's calibration curves and sweat volume capacity.

A. Capacitive SR Sensor Simulation

Different sensor shapes have been simulated using COMSOL multiphysics to show the robustness of the capacitive SR sensor design. We divide the simulation into two parts. We use a two-phase, phase field model in the first simulation to track the sweat-air interface. In this simulation, we determine the volume of sweat inside the channel over time. Microfluidic channel of width, $d_d = 1000\ \mu m$, dielectric width, $d_d = 100\ \mu m$ and thickness, $t_c = 164\ \mu m$. Density of 1000 kgm^{-3}, viscosity of $8.9 \times 10^{-4}\ Pas$, dielectric constant of $80\epsilon_0$ are used for simulating the sweat. For air, we use density of 1.225 kgm^{-3}, viscosity of $1.81 \times 10^{-5}\ Pas$, and dielectric constant of 1. In the second part of the simulation, we use AC/DC electrostatic simulation to determine the change in capacitance with varying volumes inside the channel. The dielectric constant of the encapsulation $\epsilon_d = 3$ is used in this simulation. For electrostatic simulation, the reference impedance is set to 50 Ω. One of the parallel plate capacitors' electrodes is grounded, and the other electrode is defined as a terminal with a high potential of 1 V. Fig. 2. B shows the electrostatic simulation setup. Incorporating the results from electrostatic and time-dependent simulations, we determine the capacitance change with time for different SR inputs. Since the sweat concentration is kept fixed for the simulation, the fixed dimension capacitor value does not change over time. However, during the exercise, as the sweat ion concentration changes, the value from this fixed dimension capacitor will change accordingly.

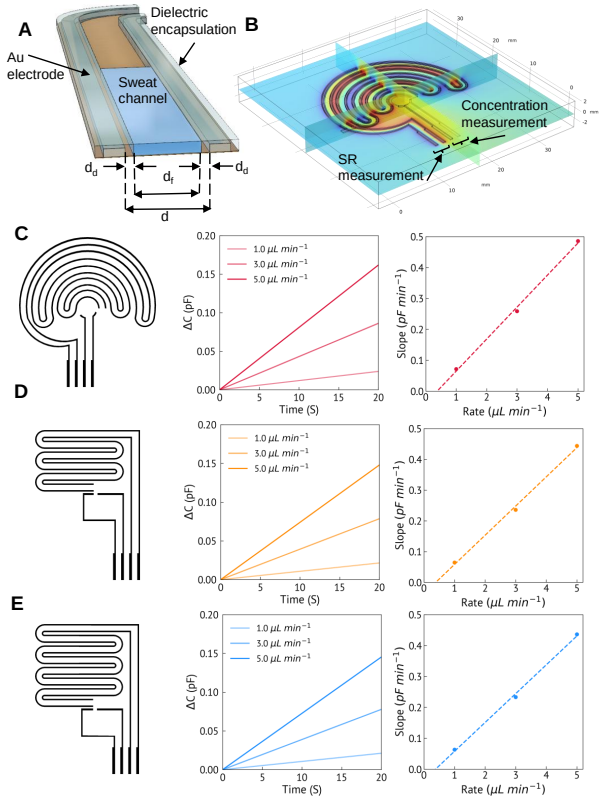

Fig. 2. **Simulation of different SR sensor designs**. (**A**) Analytical modeling setup. (**B**) Simulation Setup. Simulated change in capacitance and calibration curve for (**C**) circular design, (**D**) design with three serpentine structures, and (**E**) design with four serpentine structures.

We simulated three different designs. The first design is a circular pattern. The total volume capacity of this design is 17.5 μL. The second and the third designs have the same serpentine structures. The second design with three serpentine structures has a total capacity of 11.0 μL, and the third design with four serpentine structures has a capacity of 15.0 μL. From Fig. 2 C and D, the calibration curves are different as the designs are different. However, while we change the design by increasing the number of serpentine structures to increase the sweat channel's capacity, the calibration curve's slope remains the same, as shown in Fig. 2 D and E. These findings conclude that, depending on the application, we can increase the volume by lengthening the serpentine structure. While doing so, we can keep the same calibration curve. The circular design will be better for area efficiency. This design offers a higher volume in our SR channel while keeping the area small.

B. Sensor Fabrication

We use a flexible substrate (Xenomax) for sensor fabrication. This substrate is hydrophilic. Parallel plate gold (Au) electrodes are fabricated by inkjet printing for two sets of capacitance measurements. A dielectric encapsulation has been used to isolate the Au electrodes from direct contact with the sweat in the channel. The sweat sensor channel is fabricated by patterning a double-sided tape (3M™ Microfluidic Diagnostic Tape 9965), and for the cover, hydrophilic transport film (3M™ 9984 Diagnostic Microfluidic Surfactant Free Fluid Transport Film) is used. Univeral Laser Systems VLS6.75 patterns both the microfluidic channel and cover. Patterned microfluidics channel and cover are assembled with inkjet-printed Au electrodes to conclude the sensor fabrication. The hydrophilic substrate and cover create a capillary force to direct the sweat inside the channel. Fig. 3 A-C shows the fabrication steps. Fig. 3 D shows the fabricated sensor patch while the bar represents 3 mm. Our fabricated sensor has electrode width of 250 μm, encapsulation width of 40 μm, channel width of 850 μm and thickness of 164 μm.

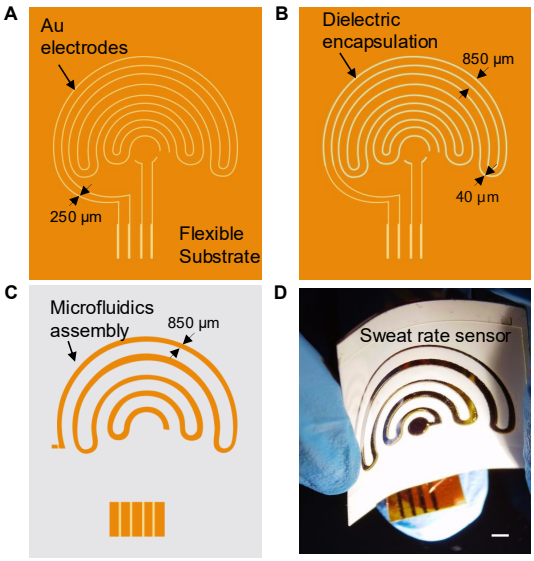

Fig. 3. **SR sensor fabrication**. (**A**) Inkjet printing the nanoparticle Au (250 μm) ink on a flexible polyimide substrate. (**B**) Inkjet printed dielectric encapsulation(40 μm) of Au electrodes. (**C**) Microfluidics channel (850 μm) and cover are patterned by a CO_2 laser and assembled on top of the inkjet printed electrodes. (**D**) Fabricated sensor patch. The bar represents 3 mm.

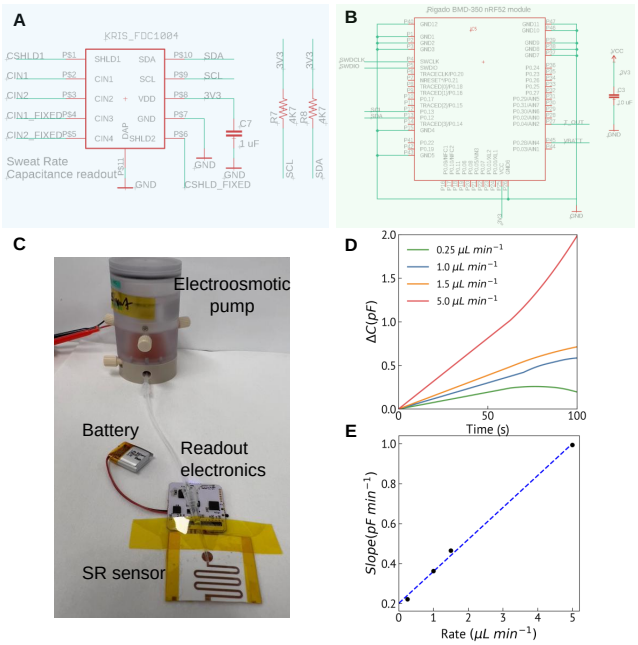

Fig. 4. **Readout electronics and calibration curve for SR sensor**. (**A**) Circuit design for reading the capacitance from two different parallel plate capacitance. (**B**) Circuit design for nRF52832 to enable wireless data transfer between the readout electronics and phone app. (**C**) Experimental setup showing the electroosmotic pump, readout electronics, battery, and the SR sensor patch. (**D**) Change in capacitance with time at different rates. (**E**) Calibration curve determined by calculating slopes (from the linear portion of Fig. 4 E) at different rates.

III. RESULTS

A. System Design and Calibration

We design the readout electronics and custom Android phone application (in the Cordova platform) for the wearable SR sensor patch. For electronics, an FDC1004 capacitance-to-digital converter measures the capacitance of two sets of parallel plate capacitors (Fig. 4 A). CIN1 and CIN2 pins measure the capacitance for the SR sensor, and CIN3 and CIN4 measure the fixed capacitance for evaluating sweat concentration. This FDC1004 is interfaced with the Bluetooth transceiver nRF52832 to streamline the display of SR in the Android phone (Fig. 4 B). The sensor is powered by a rechargeable lithium-polymer battery (3.7 V, 80 mA), which can continuously be used for 7 hours.

The design with three serpentine structures has been used for measuring the calibration curve of SR measurement. Fig. 4 C shows the experimental setup. We use an electroosmotic pump (TAKASAGO ELECTRIC, INC) to vary the rate of an artificial sweat and input this into the channel inlet of our sensor. This artificial sweat is a mixer of 10 mM NaCl, 3 mM KCl, 0.2 mM $CaCl_2$, and 0.02 mM $MgCl_2$ in DI water. Our sensor is connected to the PCB board which measures the capacitance and send it to a phone application. Fig. 4 D represents the change in capacitance with time over different input flow rates from 0.25 $\mu L\ min^{-1}$ to 5.0 $\mu L\ min^{-1}$. The calibration curve of Fig. 4 E is determined by calculating the slope from the

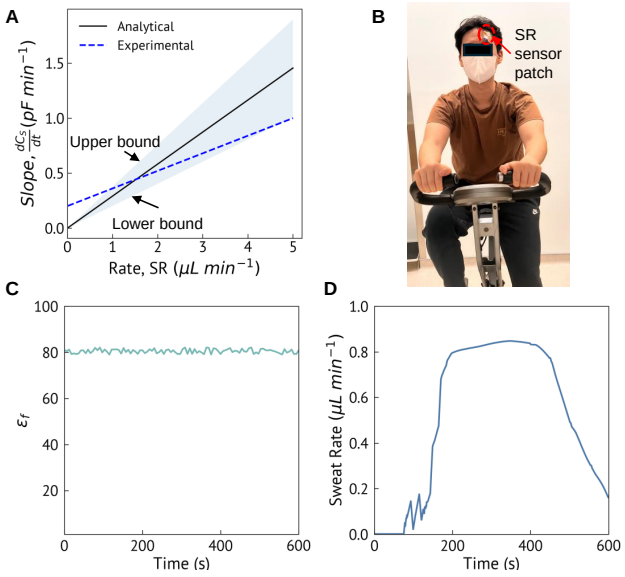

Fig. 5. **On-body SR measurement**. (**A**) Dielectric constant dependent calibration curve. (**B**) Continuous SR measurement while the participant is exercising. (**C**) Sweat concentration from fixed dimension capacitor. (**D**) Sweat concentration dependent continuous SR measurement.

linear portion (0 to 60 s) of Fig. 4 D at each input rate. This SR sensor can operate until the channel is filled.

B. On-body SR Measurement

Fig. 5 A shows the variation in the calibration curve using the equation 1. The experimentally determined calibration curve is from Fig.4 E. Here, $d_d = 850\ \mu m$, dielectric width, $d_d = 40\ \mu m$ and thickness, $t_c = 164\ \mu m$ and ϵ_f is varied from $30\epsilon_0$ to $1000\epsilon_0$. Fig. 4 E coincides with the lower bound of the calibration curve. It coincides with the lower bound because we used the lower physiological range for the concentration of the sweat analytes in artificial sweat solution. We use this sweat concentration dependent calibration curve to measure the SR. A double-sided medical tape is used to wear the SR sensor patch on the forehead, as shown in Fig. 5 B. For exercise, a stationary bike is used. From the fixed dimension capacitor, the sweat concentration is measured, and this value is used to choose the calibration curve for SR measurement in Fig. 5 C and D. We continuously measure the SR for 600 s. Initially, it takes some time for the participant to start sweating. The SR increases around 0.8 $\mu L\ min^{-1}$ and starts to decrease at around 500 s.

IV. CONCLUSION

We demonstrate a custom-made wearable sensor system that can effectively account for the variation in sweat concentration while measuring the SR. Our solution streamlines the changes in the designs of the SR sensor patch depending on the application requirements. The small and customized printed circuit board enables Bluetooth communication with Android phones. Custom phone applications display real-time SR data for the user's convenience. We used only the lower concentration artificial sweat to calibrate the SR sensor patch. In the future, the ion concentration can be changed to get the whole physiological range for the calibration curve. Overall, our sweat concentration-dependent measurement paved the way for precise measurement of SR for real-time human perspiration monitoring.

ACKNOWLEDGMENT

This work was supported in part by the USC Viterbi School of Engineering and NIH. Grant Number: 1R61MH135407-01.

REFERENCES

[1] W. Gao, S. Emaminejad, H. Y. Y. Nyein, S. Challa, K. Chen, A. Peck, H. M. Fahad, H. Ota, H. Shiraki, D. Kiriya *et al.*, "Fully integrated wearable sensor arrays for multiplexed in situ perspiration analysis," *Nature*, vol. 529, no. 7587, pp. 509–514, 2016.

[2] M. Ferdoushi, M. S. Islam, W. Cai, S. L. Galindo, M. F. Hassan, and Y. Khan, "Fully-printed sensor based extended gate field effect transistors for wireless monitoring of potassium and ammonium ions," in *2024 IEEE SENSORS*. IEEE, 2024, pp. 1–4.

[3] J. Xiao, C. Fan, T. Xu, L. Su, and X. Zhang, "An electrochemical wearable sensor for levodopa quantification in sweat based on a metal–organic framework/graphene oxide composite with integrated enzymes," *Sensors and Actuators B: Chemical*, vol. 359, p. 131586, 2022.

[4] H. L. Webster and C. A. Rundell, "Laboratory diagnosis of cystic fibrosis," *CRC Critical Reviews in Clinical Laboratory Sciences*, vol. 18, no. 4, pp. 313–338, 1982.

[5] K. Sato, W. Kang, K. Saga, and K. Sato, "Biology of sweat glands and their disorders. i. normal sweat gland function," *Journal of the American Academy of Dermatology*, vol. 20, no. 4, pp. 537–563, 1989.

[6] N. Davis, J. Heikenfeld, C. Milla, and A. Javey, "The challenges and promise of sweat sensing," *Nature Biotechnology*, pp. 1–12, 2024.

[7] S. Shirreffs and R. Maughan, "Whole body sweat collection in humans: an improved method with preliminary data on electrolyte content," *Journal of Applied Physiology*, vol. 82, no. 1, pp. 336–341, 1997.

[8] L. B. Baker, J. R. Stofan, A. A. Hamilton, and C. A. Horswill, "Comparison of regional patch collection vs. whole body washdown for measuring sweat sodium and potassium loss during exercise," *Journal of Applied Physiology*, 2009.

[9] D. M. Sletten, S. D. Weigand, and P. A. Low, "Relationship of q-sweat to quantitative sudomotor axon reflex test (qsart) volumes," *Muscle & Nerve: Official Journal of the American Association of Electrodiagnostic Medicine*, vol. 41, no. 2, pp. 240–246, 2010.

[10] L. B. Baker, J. B. Model, K. A. Barnes, M. L. Anderson, S. P. Lee, K. A. Lee, S. D. Brown, A. J. Reimel, T. J. Roberts, R. P. Nuccio *et al.*, "Skin-interfaced microfluidic system with personalized sweating rate and sweat chloride analytics for sports science applications," *Science advances*, vol. 6, no. 50, p. eabe3929, 2020.

[11] A. T. Iftekhar, J. C.-T. Ho, A. Mellinger, and T. Kaya, "3d modeling and characterization of a calorimetric flow rate sensor for sweat rate sensing applications," *Journal of Applied Physics*, vol. 121, no. 9, 2017.

[12] A. Brueck, T. Iftekhar, A. B. Stannard, K. Yelamarthi, and T. Kaya, "A real-time wireless sweat rate measurement system for physical activity monitoring," *Sensors*, vol. 18, no. 2, p. 533, 2018.

[13] P. Salvo, F. Di Francesco, D. Costanzo, C. Ferrari, M. G. Trivella, and D. De Rossi, "A wearable sensor for measuring sweat rate," *IEEE Sensors Journal*, vol. 10, no. 10, pp. 1557–1558, 2010.

[14] J. K. Sim, S. Yoon, and Y.-H. Cho, "Wearable sweat rate sensors for human thermal comfort monitoring," *Scientific reports*, vol. 8, no. 1, p. 1181, 2018.

[15] H. Y. Y. Nyein, L.-C. Tai, Q. P. Ngo, M. Chao, G. B. Zhang, W. Gao, M. Bariya, J. Bullock, H. Kim, H. M. Fahad *et al.*, "A wearable microfluidic sensing patch for dynamic sweat secretion analysis," *ACS sensors*, vol. 3, no. 5, pp. 944–952, 2018.

[16] Z. Yuan, L. Hou, M. Bariya, H. Y. Y. Nyein, L.-C. Tai, W. Ji, L. Li, and A. Javey, "A multi-modal sweat sensing patch for cross-verification of sweat rate, total ionic charge, and na+ concentration," *Lab on a Chip*, vol. 19, no. 19, pp. 3179–3189, 2019.

[17] D.-H. Choi, M. Gonzales, G. B. Kitchen, D.-T. Phan, and P. C. Searson, "A capacitive sweat rate sensor for continuous and real-time monitoring of sweat loss," *ACS sensors*, vol. 5, no. 12, pp. 3821–3826, 2020.

[18] M. S. Islam, S. Cha, M. F. Hassan, W. Cai, T. S. Saniat, C. R. Leach, and Y. Khan, "Printed wearable sweat rate sensor for continuous in situ perspiration measurement," *Advanced Intelligent Systems*, 2024, cover Article. [Online]. Available: http://dx.doi.org/10.1002/aisy.202400927

[19] C. Anderson, Z. H. Fan, J. Richsteirr, M. Sussman, and T. Nishida, "Fabrication of 3d screen-printed micro-cavities towards sweat sensors for integrated flexible hybrid electronics," in *2024 IEEE SENSORS*. IEEE, 2024, pp. 1–4.